

# Land Surface Influence on Convective Available Potential Energy (CAPE) Change during Interstorms

LILY N. ZHANG<sup>a,b</sup>, DANIEL J. SHORT GIANOTTI<sup>b</sup>, AND DARA ENTEKHABI<sup>b</sup>

<sup>a</sup> *Department of Atmospheric Sciences, University of Washington, Seattle, Washington*

<sup>b</sup> *Ralph M. Parson Laboratory for Environmental Science and Engineering, Massachusetts Institute of Technology, Cambridge, Massachusetts*

(Manuscript received 24 October 2022, in final form 17 April 2023, accepted 21 April 2023)

**ABSTRACT:** Changes in surface water and energy balance can influence weather through interactions between the land and lower atmosphere. In convecting atmospheres, increases in convective available potential energy (CAPE) at the base of the column are driven by surface turbulent fluxes and can lead to precipitation. Using two global satellite datasets, we analyze the impact of surface energy balance partitioning on convective development by tracking CAPE over soil moisture drydowns (interstorms) during the summer, when land–atmosphere coupling is strongest. Our results show that the sign and magnitude of CAPE development during summertime drydowns depends on regional hydroclimate and initial soil moisture content. On average, CAPE increases between precipitation events over humid regions (e.g., the eastern United States) and decreases slightly over arid regions (e.g., the western United States). The soil moisture content at the start of a drydown was found to only impact CAPE evolution over arid regions, leading to greater decreases in CAPE when initial soil moisture content was high. The effect of these factors on CAPE can be explained by their influence principally on surface evaporation, demonstrating the importance of evaporative controls on CAPE and providing a basis for understanding the soil moisture–precipitation relationship, as well as land–atmosphere interaction as a whole.

**SIGNIFICANCE STATEMENT:** Land–atmosphere coupling is a long-standing topic with growing interest within the climate and modeling communities. Understanding and characterizing the feedbacks between the land surface and lower atmosphere has important implications for weather and climate prediction. One component of land–atmosphere coupling not yet fully understood is the soil moisture–precipitation relationship. Our work quantifies the land influence on one pathway for precipitation, convection, by tracking the evolution of atmospheric convective energy as soils dry between storms. Using global satellite observations, we find clear spatial and temporal trends that link summertime convective development to soil moisture content and evaporation. Our observational results provide a benchmark for evaluating how well weather and climate models capture the complex coupling between land and atmosphere.

**KEYWORDS:** Land surface; Atmosphere-land interaction; CAPE; Soil moisture; Surface fluxes; Remote sensing

## 1. Introduction

Coupling between the land and atmosphere is known to impact both weather and climate. Similar to ocean–atmosphere coupling, where the longer memory in sea surface temperatures allows for predictability and low-frequency climate variability, soil moisture can also impart both memory and predictability (McColl et al. 2017; Santanello et al. 2018). In land–atmosphere coupling, soil moisture modulates the partitioning of available energy ( $A$  as sum of net radiation and ground heat flux) between the turbulent fluxes—sensible ( $H$ ) and latent (LE) heat flux; these fluxes heat and moisten the lower atmosphere, respectively (Seneviratne et al. 2010). This surface control of heat and moisture fluxes into the atmosphere as a function of soil moisture state is a primary mechanism for land–atmosphere coupling and the surface influence on weather and climate.

Quantifying land–atmosphere coupling and its dependence on land surface and climate characteristics across the globe remains a challenge. We approach the problem using only observations, which come from multiple global remote sensing datasets. We intentionally refrain from using modeled data in our study to avoid land–atmosphere coupling behaviors that are implicitly encoded in the model parameterizations and their interactions. In this sense, our observational results serve as a benchmark for evaluating how well weather and climate models presently capture land–atmosphere interactions.

Historically, research on land–atmosphere interactions has focused on the relationship between soil moisture and precipitation due to its relevance to weather and climate prediction. However, the soil moisture–precipitation relationship is difficult to characterize, as it is the result of multiple processes (e.g., radiation partitioning, turbulence, diffusion) occurring both within the three-dimensional atmosphere and locally at the land–atmosphere interface. Depending on regional climate, the relative importance, sign, and magnitude of each process and their interactions may change. We selectively sample from remotely sensed observations to characterize the influence of observable state variables on the specific land–atmosphere interaction pathways identified for this study.

 Denotes content that is immediately available upon publication as open access.

*Corresponding author:* Lily N. Zhang, lnzhang@uw.edu

DOI: 10.1175/JHM-D-22-0191.1

© 2023 American Meteorological Society. This published article is licensed under the terms of the default AMS reuse license. For information regarding reuse of this content and general copyright information, consult the AMS Copyright Policy ([www.ametsoc.org/PUBSReuseLicenses](http://www.ametsoc.org/PUBSReuseLicenses)).

## 2. Background and study framework

### a. Background

The relationship between soil moisture and rainfall has long been theorized and qualitatively observed (Shukla and Mintz 1982). In recent decades, results from both modeling and observation-based studies have quantified the soil moisture–precipitation relationship, but with inconsistent results (Seneviratne et al. 2010). Between them, there is disagreement on the magnitude, direction, and location of the feedback. Disagreement between early observational studies can be largely attributed to the scarcity of soil moisture observations and difficulties of establishing statistical causality within the available data (Seneviratne et al. 2010; Salvucci et al. 2002). Even among modeling studies, however, there is a wide range of suggested feedbacks. As part of the Global Land Atmosphere Coupling Experiment (GLACE; Koster et al. 2004, 2006; Guo et al. 2006), Koster et al. (2004) identified regions of strong soil moisture–precipitation coupling. Using 12 atmospheric general circulation models (AGCMs), the study found coupling hot spots in so-called “transitional” zones between wet and dry climates (e.g., the Great Plains in North America). Between the AGCMs, however, there was large variability, with only half of the models agreeing on there being significant coupling in North America, for example. Such large discrepancies between GCMs in characterizing the soil moisture–precipitation relationship have raised concerns about results obtained from aggregating across individual models (Orlowsky and Seneviratne 2010). Despite their limitations, there is widespread agreement that observations are necessary to evaluate model output and establish causality (Santanello et al. 2018; Seneviratne et al. 2010). Tuttle and Salvucci (2016) used remote sensing data to evaluate soil moisture–precipitation feedbacks over the continental United States and determined that coupling was not significant over the Great Plains but significant over the western and eastern United States, results that differ from Koster et al. (2004) but agree with earlier observational studies (Findell and Eltahir 2003a; Ferguson and Wood 2011). Using reanalysis data, however, Wei and Dirmeyer (2012) did find strong soil moisture–precipitation coupling in the transitional zones described by Koster et al. (2004).

One important mechanism for precipitation is convection, which occurs when parcels of air are warmed and moistened by the land surface, then rise in the atmosphere. As the parcels cool, the water vapor within them may condense—producing convective precipitation. This pathway for precipitation is well recognized and has been the topic of multiple land–atmosphere studies focusing on the dynamics of the planetary boundary layer (PBL). Most notably, Findell and Eltahir (2003b) developed the convective triggering potential (CTP)–low-level humidity index ( $HI_{low}$ ) framework, which quantifies the local atmospheric and surface conditions that determine whether the daytime PBL will reach the level of free convection (LFC). By applying the CTP– $HI_{low}$  framework to radiosonde data over the continental United States, Findell and Eltahir (2003a) were able to identify regions where surface fluxes had the greatest influence over convective

conditions. In a similar vein, Tawfik and Dirmeyer (2014) focused instead on the buoyant condensation level (BCL) to develop the heated condensation framework (HCF). Both frameworks introduce diagnostics to predict the chance of convection initiation based on morning atmospheric conditions and soil moisture content. However, more recent studies (Ferguson and Wood 2011; Wakefield et al. 2021) have demonstrated the limitations of such metrics and introduced modifications to address them. In addition, other studies such as Klein and Taylor (2020) show that soil moisture can also impact convection and rainfall nonlocally through remotely triggered mesoscale convective systems (MCSs). Therefore, the applicability of the aforementioned frameworks toward predicting convection, particularly on a global scale, continues to be a topic of ongoing discussion.

### b. Study framework

In this study we focus on the land surface influence on precursors to convective precipitation. Our analysis is based solely on observations, in order to avoid any bias toward model constructs. We examine parcels at the base of the atmosphere over land surfaces, where latent and sensible heat fluxes provide moisture and heat to the overlying column. Specifically, we examine the development of the convective available potential energy (CAPE). CAPE represents the specific amount of energy available for convection for a parcel of air. High values of CAPE generally indicate an unstable atmosphere with potential for upward motion and extreme values are observed in thunderstorms and other severe weather systems. Lifted parcels will also often encounter a region where they become negatively buoyant and sink back down to the surface. The specific and vertically integrated amount of energy that causes this negative buoyance is referred to as convective inhibition (CIN).

In addition to being commonly used in models and in weather prediction, CAPE is highly relevant to land–atmosphere interactions due to its replenishment by surface turbulent fluxes. Emanuel (1994) showed that the time rate of change in CAPE could be approximated as

$$\frac{\partial}{\partial \tau} \text{CAPE}_i \cong (T_i - T_{\text{LNB}_i}) \frac{\partial s_i}{\partial \tau} - \int_{z_i}^{z_{\text{LNB}_i}} \left( \frac{g \dot{Q}}{c_p T} - \frac{g}{\theta} \mathbf{V}_r \cdot \nabla \theta - N^2 \omega \right) dz \quad (1)$$

for a parcel  $i$ , where changes in CAPE are the result of radiative cooling ( $\dot{Q}$  in the second term), horizontal and vertical convergence (remainder of the second term), and changes in the parcel’s entropy ( $\partial s_i / \partial \tau$ ). The parcel temperature ( $T$ ) and vertical position ( $z$ ) are subscripted with  $i$  for origin and LNB for the associated level of neutral buoyancy. The time coordinate  $\tau$  is time in the reference frame of the parcel as it moves within the subcloud layer. The term  $\mathbf{V}_r$  is the horizontal velocity vector,  $\omega$  is the vertical velocity in pressure coordinates,  $N$  is the Brunt–Väisälä frequency,  $\theta$  is the potential temperature,  $c_p$  is the specific heat capacity, and  $g$  is the gravitational acceleration;  $\dot{Q}$  is the radiative heating rate.

Emanuel (1994) shows that the radiative and convergence terms [second term in (1)] are small compared to the first term (change in parcel entropy), which is driven by surface latent and sensible heat fluxes. Changes in parcel entropy over the depth of the cloud sublayer ( $\Delta z_b$ ) are related to turbulent fluxes by the following expression:

$$\begin{aligned} \frac{\partial s_i}{\partial \tau} &\sim \frac{C_D L_v |V_a| (q_s - q_i) + C_D c_p |V_a| (T_s - T_i)}{T_i \Delta z_b} \\ &= \frac{\text{latent} + \text{sensible heat flux}}{T_i \Delta z_b}, \end{aligned} \quad (2)$$

where  $C_D$  is the turbulent transfer coefficient,  $L_v$  is the latent heat of vaporization for water,  $|V_a|$  is typical anemometer-level wind speed,  $q$  is the specific humidity, and subscript  $s$  denotes the surface. Combining (1) and (2), increases in convective potential as measured by CAPE are driven by increases in parcel entropy ( $s_i$ ) which, in turn, is increased through latent and sensible heat flux. This relationship between CAPE and surface fluxes provides a framework for analyzing the linkage between soil moisture and convective precipitation potential. This serves as the foundation for the following analyses.

Despite the aforementioned contributions from surface fluxes, the current leading theory for CAPE evolution in the midlatitudes attributes CAPE buildup to advection of warm moist air (i.e., the advection hypothesis; Carlson and Ludlam 1968; Yang and Shu 1985). Advection is represented by the convergence terms in Eq. (1). A recent study from Tuckman et al. (2023), however, used backward Lagrangian tracking of parcels to show that boundary layer moistening through surface latent heat flux—as opposed to advection—is the primary contributor to CAPE buildup in the midlatitudes.

Because of its relevance to severe weather, a growing body of work has examined the impact of climate change on CAPE. The results of these studies can often be linked to low-level processes, providing additional evidence for the importance of the relationship between CAPE and the surface. Taszarek et al. (2021) evaluated the global climatology of CAPE over the past four decades but found disagreement between reanalysis and rawinsonde data on the direction of the mean trend. Among climate models, however, there is widespread agreement that CAPE is expected to increase into the future as a result of anthropogenic forcing (Tippett et al. 2015). Notably, Diffenbaugh et al. (2013) used CMIP5 (Coupled Model Intercomparison Project phase 5) projections to determine that robust increases in mean CAPE were driven by increases in low-level moisture. Similarly, Chen et al. (2020) simulated future CAPE using version 4 of the Community Climate System Model (CCSM4) and concluded that increases in CAPE resulted from increases in low-level humidity. These projected changes in humidity are due in part to the increased saturated vapor pressure of warmer future atmospheres, but realized increases in humidity over land also require sufficient moisture supply from soils.

In our study, we focus on the near-surface atmospheric energetics during surface drydowns, interstorm periods over

which turbulent heat fluxes heat and moisten the lower atmosphere. During drydowns, surface latent and sensible heat flux partitioning variably drives changes in near-surface moist enthalpy (ME). CAPE, when combined with the atmospheric profile of static stability, then determines the potential for convection and precipitation. We take drydowns to be a fundamental unit of time for land–atmosphere interactions and use observations to track the time evolution of ME and CAPE over them. Rather than delve into the dynamical processes that determine the chance of convection and precipitation on a given day, we try to answer a more fundamental question: what happens to CAPE between storms? Specifically, we analyze whether CAPE and ME increase or decrease over drydowns and how their behavior depends on regional hydroclimate. In addition, we assess the impact of initial soil moisture conditions on the rate of CAPE and ME change during drydowns. Answering these questions will provide a better mechanistic understanding of the land surface's influence on convective development and its empirical representation across space and land surface state.

### 3. Methods

#### a. Datasets

##### 1) SOIL MOISTURE DATA

Global surface soil moisture estimates used to identify drydown periods and drydown initial conditions are based on the Soil Moisture Active Passive (SMAP) microwave radiometer measurements. The SMAP version 7 dataset provides global soil moisture estimates every two to three days at 36-km posting (O'Neill et al. 2020). The SMAP satellite was launched in January 2015 and data is available from March 2015 onward. We use SMAP observations from March 2015 to November 2021 in our study, with some measurements discarded based on their retrieval quality assessment flag. Discarded measurements include those performed over snow and ice, mountainous topography, open water, urban areas, and forest vegetation with greater than  $5 \text{ kg m}^{-2}$  water content (Entekhabi et al. 2014). Colliander et al. (2021) provide assessment of the SMAP surface soil moisture product by comparing it to in situ ground stations. Across the regions included in this study, the error standard deviation of the SMAP soil moisture product is estimated to be better than 4% volumetric.

##### 2) METEOROLOGICAL DATA

Global temperature, humidity, and pressure data were obtained from the Atmospheric Infrared Sounder (AIRS) instrument (AIRS Project 2019; Susskind et al. 2014). AIRS version 7 provides daily atmospheric profiles and surface values for the aforementioned variables at  $1^\circ$  resolution. The AIRS instrument is mounted on a polar-orbiting platform (EOS-Aqua) and takes measurements along the satellite's ascending and descending orbits. Our study focuses on measurements from the ascending orbit, which observes locations at the midday 1330 local time. The length of available AIRS observations is much longer than that of SMAP; as a result, we only used a portion of the AIRS dataset from the time period

of available SMAP measurements (March 2015–November 2021). Sun et al. (2021) assess the near surface AIRS temperature and specific humidity products using triple-collocation with multiple data sources. They find that the AIRS products are susceptible to error in the tropics. These are largely overlapping with the forested regions where the soil moisture data product is not used, i.e., overlapping exclusion zones. For more information on the retrieval accuracy of AIRS in a similar context, see Ferguson and Wood (2011).

### b. Data processing

#### 1) CAPE, CIN, AND MOIST ENTHALPY CALCULATIONS

Midday CAPE values were computed for each 1° grid cell using AIRS temperature, humidity, and pressure data for each day from March 2015 to November 2021. By default, the AIRS profile contains measurements at every 100 hPa pressure level, beginning with sea level pressure (1000 hPa); however, the real surface is not always at 1000 hPa. To form the complete atmospheric profile for each variable, we appended surface values (also provided by AIRS) to the start of the pressure level data for a surface-based calculation. From the atmospheric profile, we were also able to determine the daily midday convective inhibition (CIN).

Additionally, we computed moist enthalpy (ME), defined as the moist static energy of air parcels at the surface:

$$\text{ME} = c_p T + Lq \quad (3)$$

from the surface air temperature ( $T$ ) and specific humidity ( $q$ ). The constants  $c_p$  and  $L$  denote the specific heat at constant pressure (for dry air) and the latent heat of vaporization, respectively. Moist enthalpy has two components: the sensible ( $c_p T$ ) and latent ( $Lq$ ) heat content of the parcel. The land surface contributes to moist enthalpy through surface sensible heating and evaporation (i.e., latent heat flux). Radiative fluxes, lateral advection, and vertical entrainment also influence the evolution of ME and its constitutive terms.

All necessary calculations were performed using the MetPy package in Python (May et al. 2022).

#### 2) SMAP REGRIDDING

Soil moisture data from SMAP (36-km grid) was aggregated to the 1° AIRS grid in order to match CAPE to soil moisture values for drydown identification. To accomplish this, we considered all available SMAP measurements contained within a 1° AIRS grid cell for each day and calculated the area of the grid cell covered by the SMAP swath. If at least 50% of the grid cell's total area was observed by SMAP, the soil moisture value for that day was set as the average of all enclosed SMAP measurements.

### c. Drydown analysis

#### 1) WARM SEASON DEFINITION

We evaluate drydowns for the summer months (Dong et al. 2022), when we expect land–atmosphere coupling to be strongest (within the context of our study). Because of limited

enthalpy flux from cold land surfaces, CAPE is typically close to zero in the midlatitudes for all other seasons. Traditionally, land–atmosphere coupling studies have focused on summer climate due to the more dominant influences of internal variability and large-scale precipitation on the climate in other months. Convective precipitation is also predominantly a feature of the warm season for a location. As such, we defined a “warm season” for each hemisphere and only evaluated drydowns occurring in those months. The warm season extends from the month (inclusive) of the summer solstice to the month of the fall equinox (June–September in the Northern Hemisphere and December–March in the Southern Hemisphere).

#### 2) DRYDOWN IDENTIFICATION

Fundamentally, drydowns are interstorm periods during which soil moisture is not strongly affected by precipitation infiltration. Dong et al. (2022) used this working definition of drydowns to develop an algorithm that identifies and removes soil moisture anomalies caused by precipitation—leaving only the drydown intervals. We applied the algorithm from Dong et al. (2022) to the full length of the (regridded) warm season soil moisture time series for each grid cell and took each instance of a drydown to be one “event.”

Within a drydown event, days are numbered starting from  $t = 0$  (beginning of each drydown) to  $n - 1$ , with  $n$  being the total length of the drydown (in days). Corresponding CAPE values (see section 3b) are stored for each day  $t$ , forming a time series of CAPE over the course of that drydown.

We compute mean values of CAPE, CIN, and ME for all drydown events by averaging across all drydown samples in a grid cell or region. The result is mean (and the corresponding standard error) CAPE, CIN, and ME for each location at times  $t = 0, 1, 2, \dots, n - 1$ . For this averaged time series, we only considered days up to  $t = 8$ , after which the sample size of days 8 or longer are too few to form statistically robust estimates of mean conditions.

#### 3) $\Delta$ CAPE PER DAY SUMMARY STATISTIC

From the time series for CAPE, we extracted metrics that summarized its drydown behavior. In particular, we were interested in whether CAPE increased or decreased on average during drydowns. We focused on the change in CAPE per day:

$$\frac{\Delta \text{CAPE}}{\text{day}} = \text{CAPE}_t - \text{CAPE}_{t-1} \quad (4)$$

and computed the mean  $\Delta$ CAPE per day across all drydown days in a grid cell. Doing so for all grid cells allowed us to visualize global patterns in drydown CAPE. We also computed the mean change in moist enthalpy,  $\Delta$ ME per day, using the same methodology.

#### 4) INITIAL SOIL MOISTURE INFLUENCE

To understand how ME and CAPE evolution depends on soil moisture conditions at the start of a drydown, we

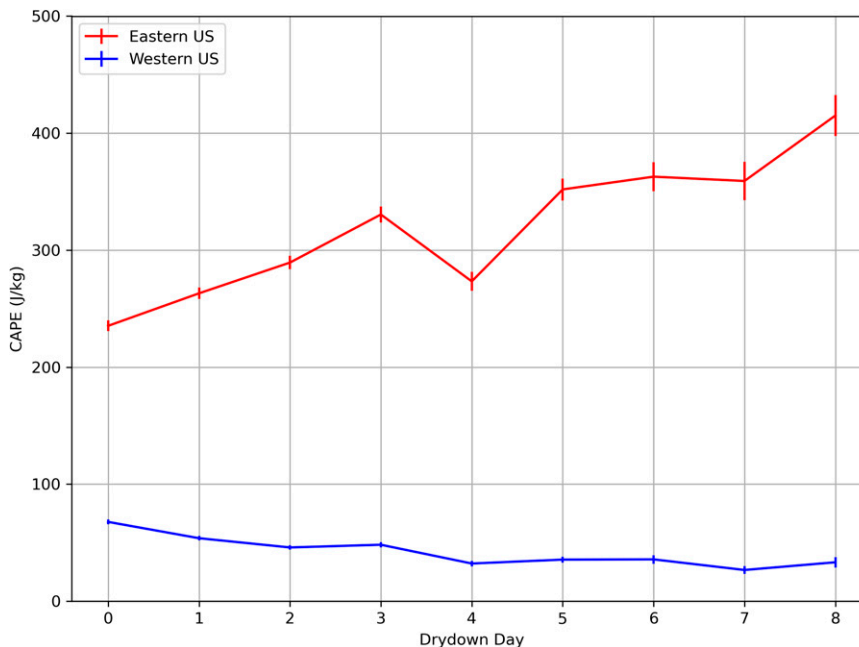


FIG. 1. Average CAPE over the course of drydowns in the eastern (red) and western (blue) contiguous United States. Vertical lines represent the 95% confidence interval of the mean.

identified the local 25th and 75th percentile of initial values within a grid cell and applied a “tag” to drydowns that were above the 75th or below the 25th. Drydowns with the tag “sm25” have initial soil moisture values below the 25th percentile (i.e., dry scenario) and, conversely, “sm75” denotes the wettest drydowns, within the climatology of each grid cell. The aforementioned  $\Delta$ CAPE per day and  $\Delta$ ME per day averages (above section) were then computed separately across drydowns under each tag.

#### 4. Results and analysis

To develop our understanding of drydown CAPE, we first applied our methodology to the continental United States (CONUS). Over this focus region, there is a strong east–west gradient in hydroclimate. This known divide allows us to compute regional averages and form time series plots of CAPE, CIN, and ME.

The east–west divide over CONUS separates hydroclimates where soil moisture availability has contrasting influences on surface energy balance and partitioning among its components (Akbar et al. 2018). In the arid western United States, low soil moisture content limits evaporation. In so-called “water limited” regimes, the rate of evaporation is dictated by the amount of water the ground can supply rather than the available radiative energy (Eagleson 1978; Zeppetello et al. 2019). As a result, the land surface energy balance dissipates the available energy more toward sensible heat flux and warming. In the eastern United States, where soil moisture is more plentiful, evaporation is instead “energy limited.” The soil is able to “supply” water for evaporation at a rate that exceeds the potential rate allowed by the available radiative

energy, so evaporation stays constant at the potential rate even as soil moisture decreases.

We set the east–west boundary at 105°W and separately computed the averaged time series for CAPE in each region. The boundary was chosen based on the results of Fig. 2, which we introduce later on in this section. In Fig. 1, CAPE increases on average over the course of a drydown in the eastern United States (red). In contrast, the western United States (blue) displays a slight decrease in CAPE during drydowns. From the drydown time series, we also calculated and plotted average  $\Delta$ CAPE per day over CONUS (Fig. 2). East of the 105°W meridian,  $\Delta$ CAPE per day is on average positive (red) during drydowns. In the western United States,  $\Delta$ CAPE per day is typically slightly negative (blue). These results summarize the time series trends from Fig. 1. No drydown data are available eastward from the Appalachians due to limited SMAP coverage over forest, mountainous topography, and urban areas. These constraints are detailed in section 3a(1).

Spatial differences in drydown CAPE development between the western and eastern United States can be explained by two main factors: 1) the regional hydroclimate and its characteristic evaporation regime and 2) dissipation of CAPE through dry convection in the atmospheric column.

In the western United States, the dry soil quickly runs out of water for evaporation. As a result, CAPE production decreases as the drydown progresses if moisture is the primary contributor to entropy increases in the surface parcel (we address and confirm this in the analyses below). In the East, however, the moist soil continuously supplies water at the potential evaporative rate dictated by incident radiative energy (Eagleson 1978), leading to comparatively greater increases in parcel entropy and thus CAPE throughout the drydown. The

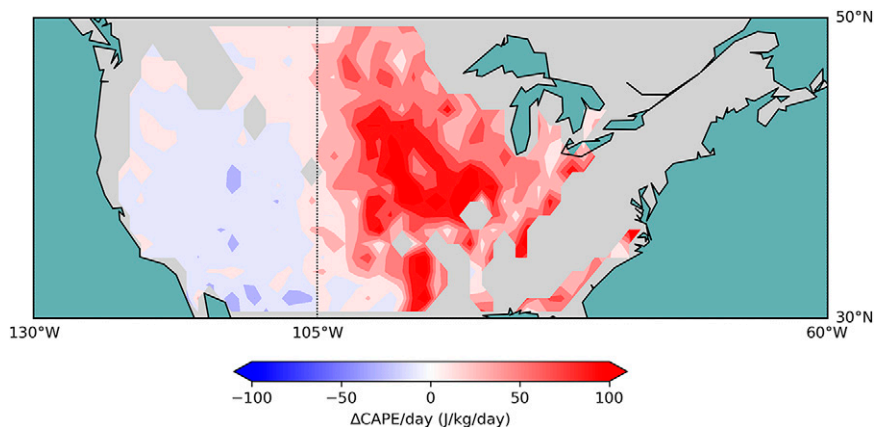


FIG. 2. Average daily change in CAPE during drydowns over the continental United States. For our study, “western United States” refers to the area west of the 105°W meridian and “eastern United States” refers to the area east of the marker. Areas shaded in gray had no results due to lack of SMAP measurements. See section 3a(1) for more details.

only exception to this trend is drydown day 4, which experiences a slight decrease in CAPE for unknown reasons. While the characteristic evaporation regimes can explain why CAPE increases are both greater and more consistent in the eastern United States, they do not explain why CAPE decreases in the western United States. If CAPE were able to accumulate in both regions, for example, we would still see an increase in total CAPE in the western United States, only at a slower rate than in the East.

The buildup over time, or lack thereof, of CAPE in both regions must be further explained by differences in the frequency of dry convection, which is reflected in the trends in

CIN during the drydown period. Figure 3 shows the average drydown time series of CIN in the eastern (red) and western (blue) United States. In the eastern United States, high CIN inhibits vertical (dry air) convective mixing and allows CAPE to build up steadily from surface fluxes over multiple days during drydowns. Conversely, in the western United States, low CIN indicates a turbulent atmosphere where dry convection frequently resets both CIN and CAPE through conversion of potential energy. Combined with the minimal contribution from surface fluxes, CAPE is unable to steadily increase from day to day as in the eastern United States and may even decrease as surface moisture supply runs out. These

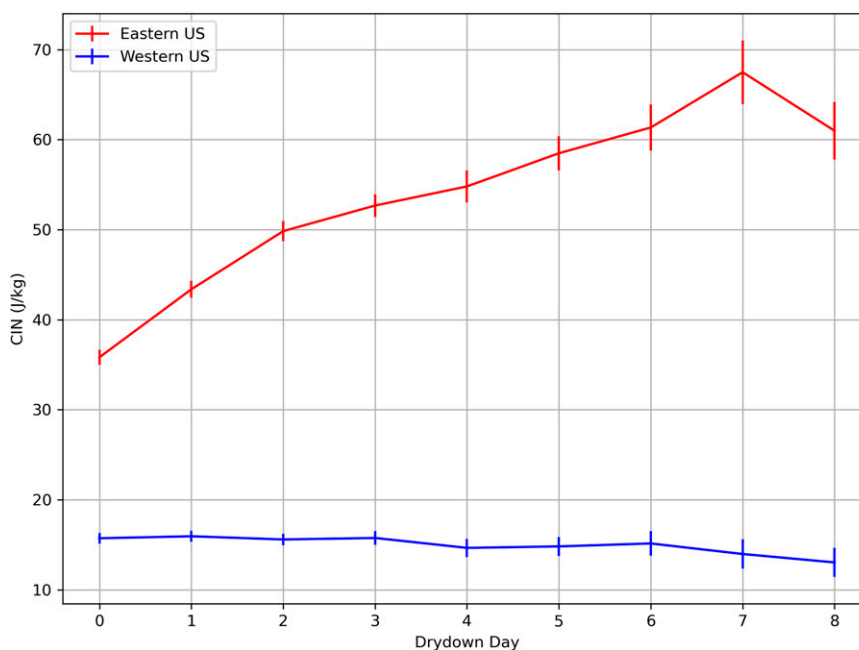


FIG. 3. Average CIN over the course of drydowns in the eastern (red) and western (blue) United States. Vertical lines represent the 95% confidence interval of the mean.

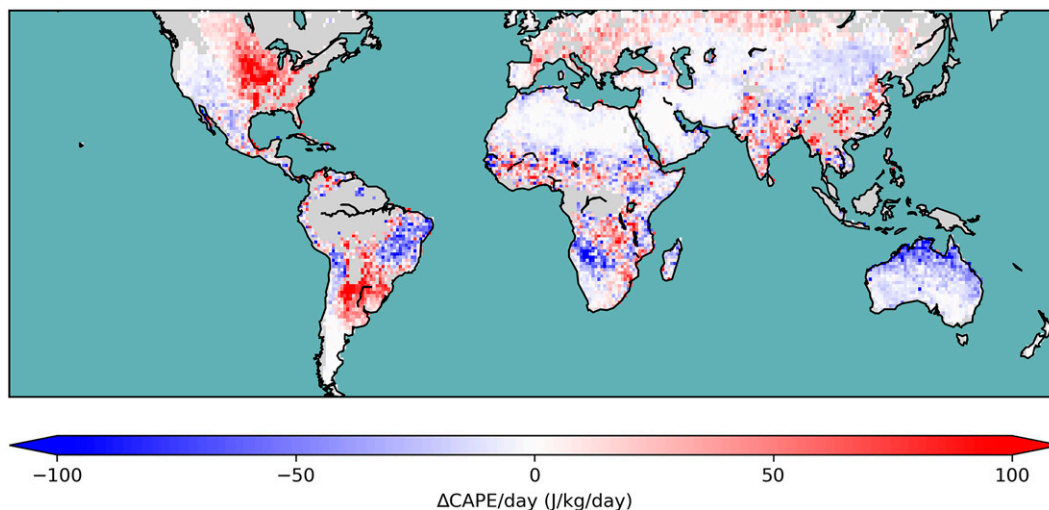


FIG. 4. Mean daily change in CAPE during drydowns across the globe.

results from CONUS suggest that insufficient moisture supply and/or insufficient convective inhibition may prevent the multi-day accumulations of CAPE between precipitation events—which is demonstrated by the  $\Delta$ CAPE per day metric.

While strong coupling between soil moisture and CAPE suggests that evaporation is the primary contributor to convective development for drydowns occurring in the western United States, it is important to note that the eastern United States also receives large advection of heat and moisture from the Gulf of Mexico. Advection may then also contribute to the larger increases in CAPE in the eastern United States. Because production of CAPE through evaporation is not sensitive to soil moisture content in the eastern United States, it is not possible to discern between the relative contributions of evaporation and advection in our results alone. However, a recent study by Li et al. (2021) found that replacing the Gulf of Mexico with land did not significantly change the amount of CAPE over North America in simulations. This, in addition to the results from Tuckman et al. (2023), provides new evidence that advection may not be the primary contributor to CAPE over CONUS. The eastern United States also differs from the western United States in its vegetation cover, which is known to impact climate. The influence of vegetation on convection, specifically, is the subject of ongoing research (Chapman and Carleton 2021).

#### a. Global patterns

Extending our analysis globally, we computed average  $\Delta$ CAPE per day for all grid cells (Fig. 4). The global evolution of CAPE during drydowns is shown to change sign depending on regional hydroclimate. As shown earlier (Fig. 2), the eastern United States is noticeably red—indicating strong increases in CAPE during drydowns. Other hotspots of positive  $\Delta$ CAPE per day include parts of South America and East Asia. The red portion of South America corresponds to the Río de La Plata basin, which experiences a humid subtropical climate. Similarly, East Asia typically sees high humidity and

temperatures during the summer months. In general, we find that  $\Delta$ CAPE per day is positive over land regions with ample moisture supply to the base of the atmosphere through surface evaporation. In these regions CAPE builds up during drydown periods and  $\Delta$ CAPE per day is positive. Dry convection does not disturb the accumulation as evident in the buildup of CIN (Fig. 3). As a result, the land surface influence is to systematically build up CAPE until it can overwhelm the CIN buildup. A moist convective event results from these systematic changes during drydowns over multiple days. However, the aforementioned regions also experience large advection of heat and moisture from surrounding bodies of water, which can also increase CAPE. Additionally, vegetation, which may impact soil moisture–convection coupling (Chapman and Carleton 2021), has greater coverage in more humid climates. As a result, we cannot conclude that this is a positive feedback due solely to land–atmosphere interactions across these energy-limited evaporation regime land regions that also experience large advection and contain more vegetation.

Conversely,  $\Delta$ CAPE per day appears to be on average negative (blue) or close to zero in areas such as the western United States, Middle East, Sahara, and inland Australia (Fig. 4). In these arid and semiarid climates, low moisture supply at the base of the atmospheric column as well as frequent dry convective mixing of the atmosphere inhibits the build-up of CAPE during drydowns. As the drydown extends and moisture supply from evaporation is more and more limited, the CAPE change or  $\Delta$ CAPE per day is negative during the course of drydowns. In the desert Middle East and Sahara, CAPE barely changes (white), remaining close to zero from beginning to end. Inasmuch as CAPE is a precursor to the next moist convection event, this is a negative feedback in land–atmosphere interactions across these water-limited evaporation regime land regions.

The distinct sign change of  $\Delta$ CAPE per day displayed across different regional evaporation regimes shows the hydroclimate

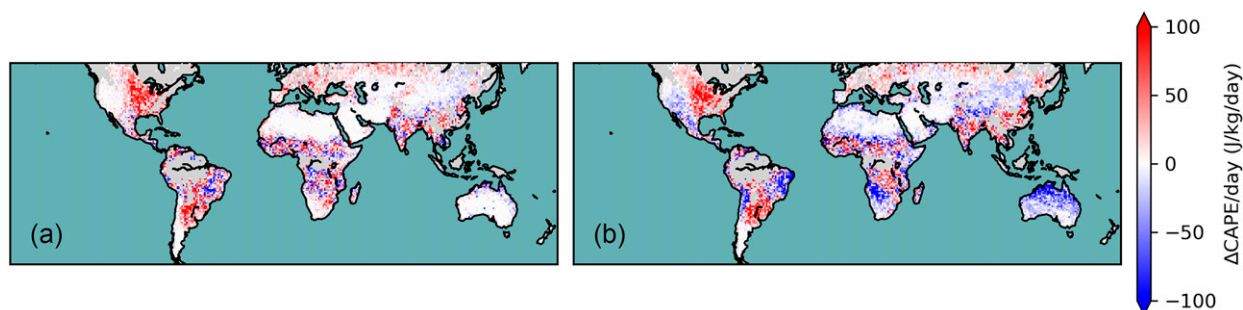


FIG. 5. Mean daily change in CAPE for drydowns in the (a) bottom 25th and (b) top 25th percentile of initial soil moisture values.

context dependence of land–atmosphere interactions. A natural question to ask is if the strength of the interactions in each region is dependent on the initial soil moisture condition at the beginning of drydowns. That is, if the local state of soil moisture (anomalously high or low) reinforces the land–atmosphere interactions that are characteristic of the region.

#### b. Initial soil moisture influence on CAPE evolution during drydowns

Figure 5 shows the result of tagging drydowns within each grid cell by their initial soil moisture values (see section 3c). Between the top and bottom 25th percentile, arid regions such as the western United States and inland Australia become noticeably more negative (blue) in the wetter 75th percentile scenario when compared to the 25th percentile. In the 25th percentile of initial soil moisture conditions,  $\Delta\text{CAPE}$  per day averages to zero (white).

In general, initial soil moisture conditions appear to have the greatest impact on CAPE evolution in regions where  $\Delta\text{CAPE}$  per day is either negative or zero on average. As noted above, these regions correspond to arid and semiarid climates. Returning to the evaporative regimes we introduced at the beginning of the section, these regions can also be classified as water-limited regimes. Since evaporation increases CAPE, it follows that drydown CAPE is most sensitive to initial soil moisture where evaporation is most sensitive to soil moisture.

In contrast, if the region evaporation regime is energy-limited, then an extra amount or a lower amount of soil moisture does not affect the evaporation rate, provided there is still sufficient moisture available for evaporation. As a result, in humid regions where  $\Delta\text{CAPE}$  per day is positive, the initial soil moisture anomaly does not affect the evolution of CAPE.

These results bear some similarities to the conclusions of Koster et al. (2004), which identified coupling between evaporation and soil moisture as a necessary condition for coupling between precipitation and soil moisture. Like Koster et al. (2004), we find that soil moisture anomalies have the strongest influence on convective development in water-limited regimes where evaporation is dependent on soil moisture. However, the study also described “suitably high” amounts of evaporation, and thus moisture, as an additional condition for coupling—placing their hotspots in more “transitional” climates such as the Great Plains. In contrast, Tuttle and Salvucci (2016)

performed an empirical study over CONUS and found feedbacks between soil moisture and precipitation were strongest over the western United States—as we found with soil moisture and CAPE feedbacks. These connections between our findings and the literature highlight the critical role that land surface–CAPE interactions play in mediating the relationship between soil moisture and precipitation.

Throughout the discussion of results so far, we have focused on the role of surface evaporation to CAPE development during drydowns. But as Eq. (2) shows, both surface sensible and latent heat flux contribute positively to the increase in the entropy of the parcel and add to CAPE over time. We return to this topic and analyze how much heating and moistening each add (separately) to the parcel energetics.

#### c. Relative contributions of heat and moisture

Delving further into the atmospheric response to evaporation, we analyzed the drydown behavior of surface parcel moist enthalpy ( $\text{ME} = c_p T + Lq$ ), which characterizes atmospheric energetic conditions at the base of the atmosphere. CAPE is the buoyant energy available to raise a parcel of air from this atmospheric boundary layer through the atmospheric profile of environmental temperature and humidity. ME is thus a link in how surface turbulent fluxes contribute to the CAPE evolution. The specific dry ( $c_p T$ ) and latent ( $Lq$ ) heat content components of moist enthalpy relate to CAPE as they are the characteristics of the originating parcel during lift to the level of free convection. Figure 6 compares the change in drydown moist enthalpy and its components between different initial soil moisture conditions.

The moist enthalpy of surface air parcels and their dry and latent heat components evolve during drydowns. The change in each depends on the land surface energy balance and partitioning of available energy into sensible and latent heat. The latter depends on the dominant evaporation regime (water or energy limited). As such, the average daily change in ME during drydowns is dependent on the evaporation regime and anomalies in soil moisture at the onset of drydowns.

As with CAPE, moist enthalpy displays the greatest difference between the high and low initial soil moisture conditions in arid and semiarid regions (Figs. 6a,b). Over the western United States, Sahara, and inland Australia,  $\Delta\text{ME}$  per day becomes more negative (blue) in the 75th percentile of initial

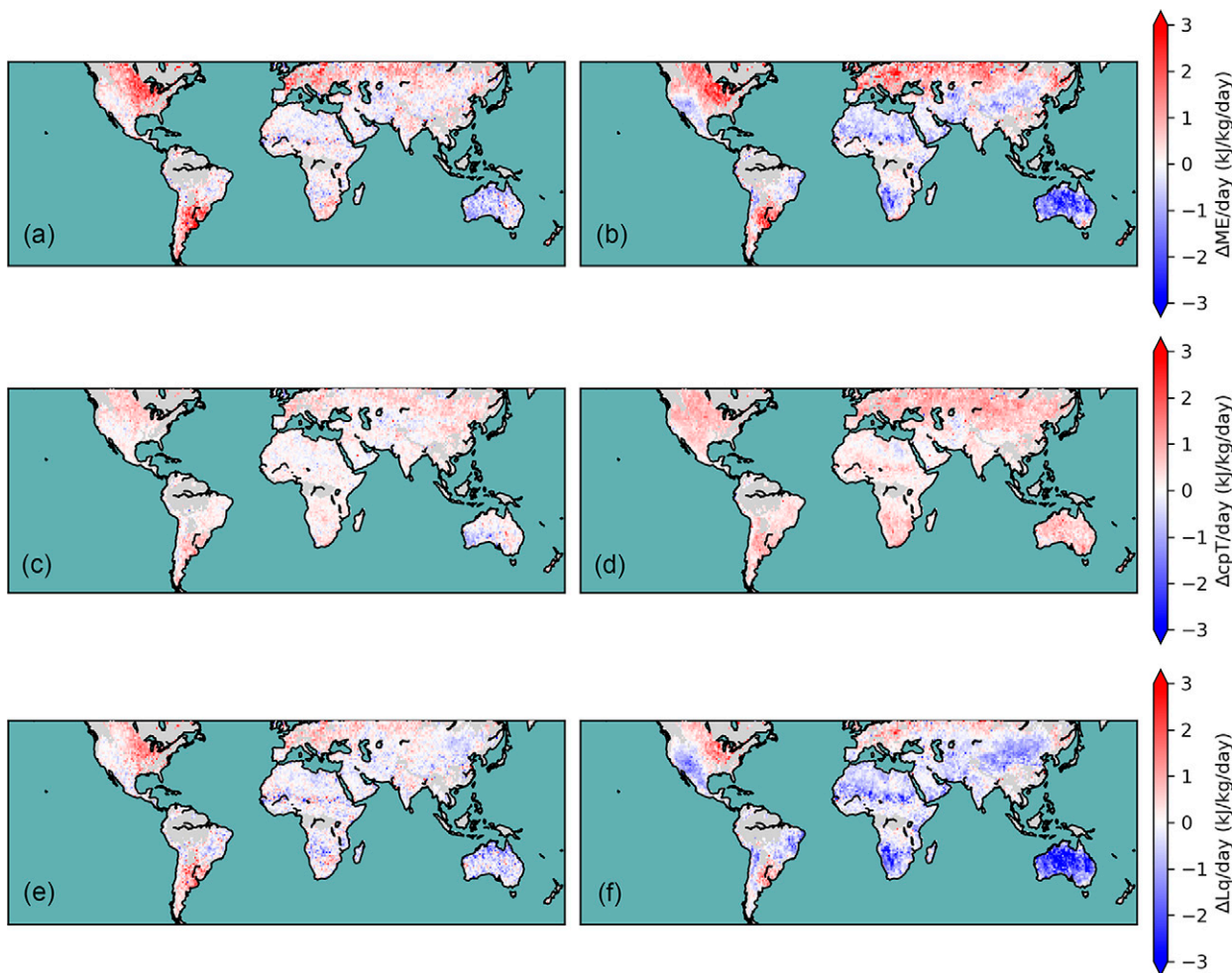


FIG. 6. Mean daily change in (a),(b) ME, (c),(d)  $c_p T$ , (e),(f)  $Lq$  for drydowns in the (left) bottom 25th and (right) top 25th percentile of initial soil moisture values.

soil moisture conditions, indicating a greater decrease in moist enthalpy as drydowns progress.

When we separated analysis of drydown moist enthalpy into its components, trends in the latent heat component appear to account for most of the magnitude of the trends seen in moist enthalpy, with the exception of the northern high latitudes (Figs. 6e,f). Particularly over the arid and semiarid regions that were most sensitive to initial soil moisture, this suggests that changes in latent heat drive changes in moist enthalpy.

To explain the patterns in  $\Delta Lq$  per day, we highlight the following: evaporation of soil moisture contributes to humidity ( $q$ ), which is the key variable in latent heat content of surface air parcels ( $Lq$ ). In arid and semiarid regions where evaporation is sensitive to soil moisture content, wetter soil (25th percentile) initially produces higher humidity (see appendix). However, as the soil runs out of moisture, surface humidity, and thus latent heat, experiences greater continuous decreases as the drydown continues. These changes in latent heat also drive  $\Delta CAPE$ . In contrast, the humidity over drier soils (75th percentile) quickly

reaches near-zero levels and stays there for the remainder of a drydown. As a result, the slope of latent heat for the entire drydown is flatter and the average  $\Delta Lq$  per day is close to zero in the dry scenario.

The nearly identical patterns produced by the soil moisture tag between  $\Delta Lq$  per day and  $\Delta CAPE$  per day suggest that changes in latent heat content account for the behavior of drydown CAPE in most regions. In arid and semiarid regions, land surface evaporation (i.e., latent heat flux) is the key contributor to changes in latent heat. However, more work is needed to understand the land surface influence in regions where 1) evaporation is not sensitive to the initial soil moisture conditions and 2) moisture supply from advection and vegetation also contribute to latent heat.

## 5. Summary and conclusions

Using global satellite products, we estimated the observed rate of change of the atmospheric column convective potential during interstorm periods. During these periods also

known as soil moisture drydowns, the land surface energy balance, which depends on available soil moisture, adjusts the dissipation of available energy through either sensible or latent heat flux. The supply of heat and moisture from these exchanges at the land–atmosphere interface affects the energetics of the overlying air parcel. The energetics of the surface air parcel, in turn, affects its convective potential (CAPE) as it is lifted up into the atmospheric column and encounters variations in buoyancy relative to the environment.

Based on these principles, we identified the patterns of land–atmosphere coupling that link the evolution of land surface soil moisture following the end of one precipitation event to the accumulation of conditions favorable to moist convection leading to the next precipitation event. In our study, we analyzed the sign and magnitude of this potential coupling by analyzing the coevolution of conditions during interstorms occurring in the summer months. Specifically, the average evolution of CAPE, CIN, moist enthalpy, and its sensible and latent heat constituents during interstorms were tracked globally using two Earth-observing satellite records.

In general, evaporation and its relative variations with soil moisture anomalies were found to be the primary driver of the evolution of the atmosphere’s convective potential. However, the magnitude of the linkage and even its sign vary geographically with the hydroclimatology of the region—specifically if it is dominated by a water-limited evaporation regime or an energy-limited evaporation regime.

In humid climates (e.g., eastern United States, South America’s Río de La Plata basin), CAPE and moist enthalpy increase on average between storms due to high amounts of soil moisture available for evaporation. Advection of heat and moisture as well as vegetation may also play a role. In drier regions (e.g., western United States, inland Australia) where soil moisture deficit limits evaporation, CAPE and moist enthalpy changes are typically small in the days following rainfall and may even decrease slightly. In summary, after rainfall, the moistening of the atmosphere at its base by evaporation dominates over sensible heating in increasing surface moist enthalpy and CAPE.

In water-limited regions, increases in the energetics of a surface parcel are inhibited by soil moisture control on the land evaporation rate. Over these regions, low soil moisture supply sufficiently constrains evaporation to prevent the build-up of convection potential between most precipitation events. The inhibition of surface parcel convection (CIN) due to negative low-level buoyancy also decreases during drydowns, causing humidity to be lost more rapidly via dry convection and horizontal advection than it is supplied from the surface. In land–atmosphere interactions, this represents a negative feedback. The observations show that the strength of this feedback varies with the state of soil moisture since when in a water-limited regime, any anomalies in soil moisture reflect corresponding anomalies in evaporation.

In energy-limited regions, the supply of moisture to surface air parcels at the base of the atmosphere with high evaporation rates results in consistent buildup of convection potential in between two precipitation events. Dry convection that can destroy buoyancy and inhibition throughout the atmospheric

column is not as dominant as it is in more arid hydroclimatic regions. As a result of the high multiday surface evaporation rate and diminished tendency of the atmospheric column toward neutral conditions, the potential for convective events increases as the drydown progresses. Because evaporation in these regions is not strongly coupled to soil moisture, this behavior is not sensitive to the soil moisture state at the start of a drydown. However, we were unable to identify a positive feedback in land–atmosphere interactions alone due to the potential contribution from advection and vegetation.

Overall, we conclude that surface fluxes, particularly evaporation, do exert significant control over convective adjustment over land. To access these pathways, we needed to use drydowns as the fundamental time period for our analysis. Our results, which are entirely based in observations and basic physical principles, provide a framework for understanding the complex near-surface processes that make up land–atmosphere coupling. Because the patterns and behaviors we found are not emergent behaviors resulting from the interaction of several modules and parameterizations within a model, they can be used as benchmarks for future work in assessing numerical weather and climate models. Our results can be easily reproduced by performing diagnostics on model data in order to test whether models are coupling land and atmospheric processes as they occur in the physical world.

*Acknowledgments.* LNZ acknowledges support by the AMS/NOAA Climate Program Office Graduate Fellowship and William and Carol Lau Term Fellowship in Atmospheric Sciences. DE and DSG acknowledge partial grant support from NASA through Jet Propulsion Laboratory/California Institute of Technology subcontract 1510842 to the Massachusetts Institute of Technology. Data and code for generating the results and figures are available from the author upon request. The authors thank Jianzhi Dong for providing the drydown identification code used in this study. Helpful discussions with Kerry Emanuel and David Battisti are also gratefully acknowledged.

*Data availability statement.* All soil moisture data (SMAP v7) used in this study are openly available from the NASA National Snow and Ice Data Center at <https://doi.org/10.5067/HH4SZ2PXSP6A>. All meteorological data (AIRS v7) used in this study are openly available from the Goddard Earth Sciences Data and Information Services Center at <https://doi.org/10.5067/UO3Q64CTTS1U>.

## APPENDIX

### **Difference in Typical Drydown Values for CAPE, Moist Enthalpy, and Moist Enthalpy Components between Soil Moisture Scenarios**

For reference, we have included the difference in typical (mean) values of CAPE, moist enthalpy, and moist enthalpy at the start of a drydown ( $t = 0$ ) between each of the soil moisture scenarios. The value plotted for each variable, with CAPE as an example, is

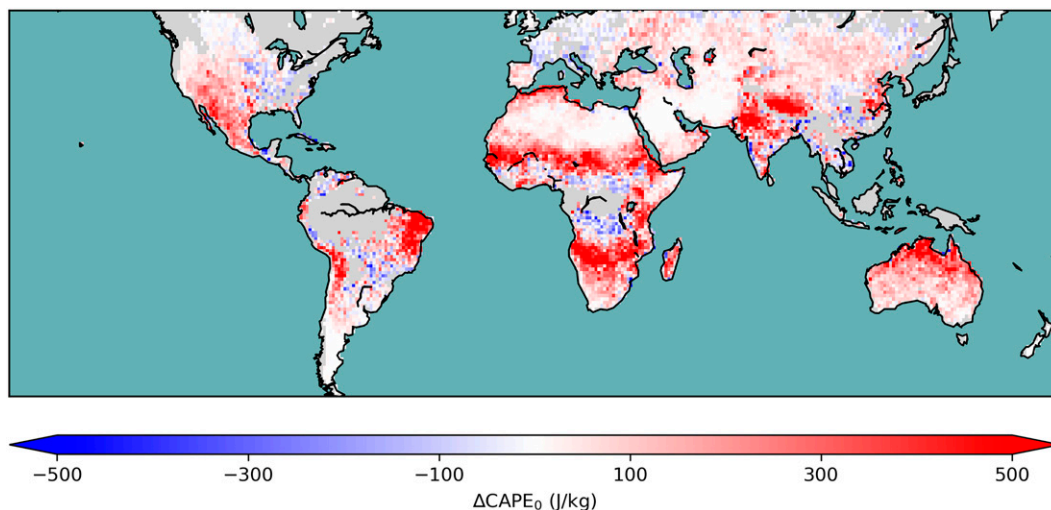


FIG. A1. Difference in CAPE at  $t = 0$  between drydowns in the top and bottom 25th percentile of initial soil moisture values. Direction of the difference is wet minus dry.

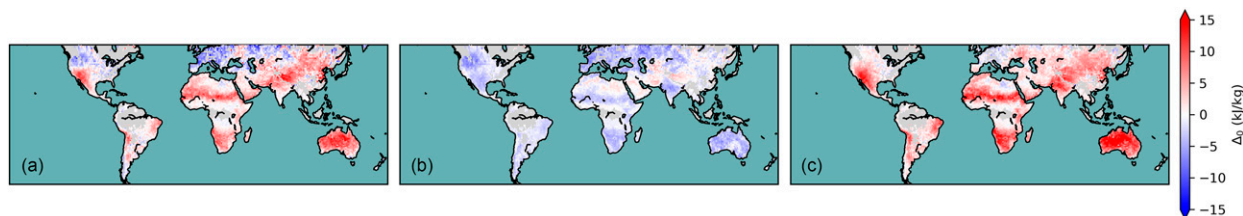


FIG. A2. Difference in (a) moist enthalpy, (b) sensible heat, and (c) latent heat at  $t = 0$  between drydowns in the top and bottom 25th percentile of initial soil moisture values. Direction of the difference is wet minus dry.

$$\Delta\text{CAPE}_0 = \text{CAPE}_{0,\text{sm}75} - \text{CAPE}_{0,\text{sm}25},$$

where  $\text{CAPE}_{0,\text{sm}75}$  and  $\text{CAPE}_{0,\text{sm}25}$  are the starting points of CAPE for drydowns in the top (wet scenario) and bottom (dry scenario) 25th percentile of initial soil moisture values. Figure A1 shows that, between the two scenarios, CAPE starts out much higher for drydowns in the top 25th percentile of initial soil moisture values—particularly in the arid and semiarid regions identified in our study. Initial moist enthalpy and latent heat are also noticeably higher in the wet scenario, with only sensible heat showing a decrease in starting values from dry to wet (Fig. A2).

#### REFERENCES

- AIRS Project, 2019: Aqua/AIRS L3 daily standard physical retrieval (AIRS-only) 1 degree  $\times$  1 degree V7.0. GES DISC, accessed 18 January 2022, [https://disc.gsfc.nasa.gov/datasets/AIRS3STD\\_7.0/summary](https://disc.gsfc.nasa.gov/datasets/AIRS3STD_7.0/summary).
- Akbar, R., D. J. S. Gianotti, K. A. McColl, E. Haghghi, G. D. Salvucci, and D. Entekhabi, 2018: Estimation of landscape soil water losses from satellite observations of soil moisture. *J. Hydrometeorol.*, **19**, 871–889, <https://doi.org/10.1175/JHM-D-17-0200.1>.
- Carlson, T. N., and F. H. Ludlam, 1968: Conditions for the occurrence of severe local storms. *Tellus*, **20A** (2), 203–226, <https://doi.org/10.3402/tellusa.v20i2.10002>.
- Chapman, C. J., and A. M. Carleton, 2021: Soil moisture influence on warm-season convective precipitation for the U.S. Corn Belt. *J. Appl. Meteor. Climatol.*, **60**, 1615–1632, <https://doi.org/10.1175/JAMC-D-20-0285.1>.
- Chen, J., A. Dai, Y. Zhang, and K. L. Rasmussen, 2020: Changes in convective available potential energy and convective inhibition under global warming. *J. Climate*, **33**, 2025–2050, <https://doi.org/10.1175/JCLI-D-19-0461.1>.
- Colliander, A., and Coauthors, 2021: Validation of soil moisture data products from the NASA SMAP mission. *IEEE J. Sel. Top. Appl. Earth Obs. Remote Sens.*, **15**, 364–392, <https://doi.org/10.1109/JSTARS.2021.3124743>.
- Diffenbaugh, N. S., M. Scherer, and R. J. Trapp, 2013: Robust increases in severe thunderstorm environments in response to greenhouse forcing. *Proc. Natl. Acad. Sci. USA*, **110**, 16 361–16 366, <https://doi.org/10.1073/pnas.1307758110>.
- Dong, J., R. Akbar, D. J. Short Gianotti, A. F. Feldman, W. T. Crow, and D. Entekhabi, 2022: Can surface soil moisture information identify evapotranspiration regime transitions? *Geophys. Res. Lett.*, **49**, e2021GL097697, <https://doi.org/10.1029/2021GL097697>.
- Eagleson, P. S., 1978: Climate, soil, and vegetation: 4. The expected value of annual evapotranspiration. *Water Resour. Res.*, **14**, 731–739, <https://doi.org/10.1029/WR014i005p00731>.

- Emanuel, K., 1994: *Atmospheric Convection*. Oxford University Press, 580 pp.
- Entekhabi, D., and Coauthors, 2014: SMAP Handbook Soil Moisture Active Passive: Mapping soil moisture and freeze/thaw from space. JPL CL14-2285, JPL Publ. 400-1567, Jet Propulsion Laboratory, 180 pp., [https://smap.jpl.nasa.gov/system/internal\\_resources/details/original/178\\_SMAP\\_Handbook\\_FINAL\\_1\\_JULY\\_2014\\_Web.pdf](https://smap.jpl.nasa.gov/system/internal_resources/details/original/178_SMAP_Handbook_FINAL_1_JULY_2014_Web.pdf).
- Ferguson, C. R., and E. F. Wood, 2011: Observed land–atmosphere coupling from satellite remote sensing and reanalysis. *J. Hydrometeorol.*, **12**, 1221–1254, <https://doi.org/10.1175/2011JHM1380.1>.
- Findell, K. L., and E. A. B. Eltahir, 2003a: Atmospheric controls on soil moisture–boundary layer interactions. Part II: Feedbacks within the continental United States. *J. Hydrometeorol.*, **4**, 570–583, [https://doi.org/10.1175/1525-7541\(2003\)004<0570:ACOSML>2.0.CO;2](https://doi.org/10.1175/1525-7541(2003)004<0570:ACOSML>2.0.CO;2).
- , and —, 2003b: Atmospheric controls on soil moisture–boundary layer interactions. Part I: Framework development. *J. Hydrometeorol.*, **4**, 552–569, [https://doi.org/10.1175/1525-7541\(2003\)004<0552:ACOSML>2.0.CO;2](https://doi.org/10.1175/1525-7541(2003)004<0552:ACOSML>2.0.CO;2).
- Guo, Z., and Coauthors, 2006: GLACE: The Global Land–Atmosphere Coupling Experiment. Part II: Analysis. *J. Hydrometeorol.*, **7**, 611–625, <https://doi.org/10.1175/JHM511.1>.
- Klein, C., and C. M. Taylor, 2020: Dry soils can intensify meso-scale convective systems. *Proc. Natl. Acad. Sci. USA*, **117**, 21 132–21 137, <https://doi.org/10.1073/pnas.2007998117>.
- Koster, R. D., and Coauthors, 2004: Regions of strong coupling between soil moisture and precipitation. *Science*, **305**, 1138–1140, <https://doi.org/10.1126/science.1100217>.
- , and Coauthors, 2006: GLACE: The Global Land–Atmosphere Coupling Experiment. Part I: Overview. *J. Hydrometeorol.*, **7**, 590–610, <https://doi.org/10.1175/JHM510.1>.
- Li, F., D. R. Chavas, K. A. Reed, N. Rosenbloom, and D. T. Dawson II, 2021: The role of elevated terrain and the Gulf of Mexico in the production of severe local storm environments over North America. *J. Climate*, **34**, 7799–7819, <https://doi.org/10.1175/JCLI-D-20-0607.1>.
- May, R. M., and Coauthors, 2022: MetPy: A meteorological Python library for data analysis and visualization. *Bull. Amer. Meteor. Soc.*, **103**, E2273–E2284, <https://doi.org/10.1175/BAMS-D-21-0125.1>.
- McColl, K. A., W. Wang, B. Peng, R. Akbar, D. J. Short Gianotti, H. Lu, M. Pan, and D. Entekhabi, 2017: Global characterization of surface soil moisture drydowns. *Geophys. Res. Lett.*, **44**, 3682–3690, <https://doi.org/10.1002/2017GL072819>.
- O’Neill, P. E., S. Chan, E. G. Njoku, T. Jackson, R. Bindlish, and J. Chaubell, 2020: SMAP L3 radiometer global daily 36 km EASE-grid soil moisture, version 7. NASA National Snow and Ice Data Center Distributed Active Archive Center, accessed 18 January 2022, <https://doi.org/10.5067/HH4SZ2PXSP6A>.
- Orlowsky, B., and S. I. Seneviratne, 2010: Statistical analyses of land–atmosphere feedbacks and their possible pitfalls. *J. Climate*, **23**, 3918–3932, <https://doi.org/10.1175/2010JCLI3366.1>.
- Salvucci, G. D., J. A. Saleem, and R. Kaufmann, 2002: Investigating soil moisture feedbacks on precipitation with tests of Granger causality. *Adv. Water Resour.*, **25**, 1305–1312, [https://doi.org/10.1016/S0309-1708\(02\)00057-X](https://doi.org/10.1016/S0309-1708(02)00057-X).
- Santanello, J. A., and Coauthors, 2018: Land–atmosphere interactions: The LoCo perspective. *Bull. Amer. Meteor. Soc.*, **99**, 1253–1272, <https://doi.org/10.1175/BAMS-D-17-0001.1>.
- Seneviratne, S. I., T. Corti, E. L. Davin, M. Hirschi, E. B. Jaeger, I. Lehner, B. Orlowsky, and A. J. Teuling, 2010: Investigating soil moisture–climate interactions in a changing climate: A review. *Earth-Sci. Rev.*, **99**, 125–161, <https://doi.org/10.1016/j.earscirev.2010.02.004>.
- Shukla, J., and Y. Mintz, 1982: Influence of land-surface evapotranspiration on the Earth’s climate. *Science*, **215**, 1498–1501, <https://doi.org/10.1126/science.215.4539.1498>.
- Sun, J., K. A. McColl, Y. Wang, A. J. Rigden, H. Lu, K. Yang, Y. Li, and J. A. Santanello, 2021: Global evaluation of terrestrial near-surface air temperature and specific humidity retrievals from the Atmospheric Infrared Sounder (AIRS). *Remote Sens. Environ.*, **252**, 112146, <https://doi.org/10.1016/j.rse.2020.112146>.
- Susskind, J., J. M. Blaisdell, and L. Iredell, 2014: Improved methodology for surface and atmospheric soundings, error estimates, and quality control procedures: The Atmospheric Infrared Sounder science team version-6 retrieval algorithm. *J. Appl. Remote Sens.*, **8**, 084994, <https://doi.org/10.1117/1.JRS.8.084994>.
- Taszarek, M., J. T. Allen, M. Marchio, and H. E. Brooks, 2021: Global climatology and trends in convective environments from ERA5 and rawinsonde data. *npj Climate Atmos. Sci.*, **4**, 35, <https://doi.org/10.1038/s41612-021-00190-x>.
- Tawfik, A. B., and P. A. Dirmeyer, 2014: A process-based framework for quantifying the atmospheric preconditioning of surface-triggered convection. *Geophys. Res. Lett.*, **41**, 173–178, <https://doi.org/10.1002/2013GL057984>.
- Tippett, M. K., J. T. Allen, V. A. Gensini, and H. E. Brooks, 2015: Climate and hazardous convective weather. *Curr. Climate Change Rep.*, **1**, 60–73, <https://doi.org/10.1007/s40641-015-0006-6>.
- Tuckman, P., V. Agard, and K. Emanuel, 2023: Evolution of convective energy and inhibition before instances of large CAPE. *Mon. Wea. Rev.*, **151**, 321–338, <https://doi.org/10.1175/MWR-D-21-0302.1>.
- Tuttle, S., and G. Salvucci, 2016: Empirical evidence of contrasting soil moisture–precipitation feedbacks across the United States. *Science*, **352**, 825–828, <https://doi.org/10.1126/science.aaa7185>.
- Wakefield, R. A., D. D. Turner, and J. B. Basara, 2021: Evaluation of a land–atmosphere coupling metric computed from a ground-based infrared interferometer. *J. Hydrometeorol.*, **22**, 2073–2087, <https://doi.org/10.1175/JHM-D-20-0303.1>.
- Wei, J., and P. A. Dirmeyer, 2012: Dissecting soil moisture–precipitation coupling. *Geophys. Res. Lett.*, **39**, L19711, <https://doi.org/10.1029/2012GL053038>.
- Yang, G., and C. Shu, 1985: Large-scale environmental conditions for thunderstorm development. *Adv. Atmos. Sci.*, **2**, 508–521, <https://doi.org/10.1007/BF02678749>.
- Zeppetello, L. R. V., D. S. Battisti, and M. B. Baker, 2019: The origin of soil moisture evaporation “regimes.” *J. Climate*, **32**, 6939–6960, <https://doi.org/10.1175/JCLI-D-19-0209.1>.